ARL-TN-1091 ● Nov 2021

# Method for Rapid Small-Scale Simulated Aluminum Alloy Castings

by Taylor Cain and Jon-Erik Mogonye

## NOTICES

### Disclaimers

The findings in this report are not to be construed as an official Department of the Army position unless so designated by other authorized documents.

Citation of manufacturer's or trade names does not constitute an official endorsement or approval of the use thereof.

Destroy this report when it is no longer needed. Do not return it to the originator.

ARL-TN-1091 ● Nov 2021

# Method for Rapid Small-Scale Simulated Aluminum Alloy Castings

**Taylor Cain and Jon-Erik Mogonye**
*Weapons and Materials Research Directorate,*
*DEVCOM Army Research Laboratory*

# REPORT DOCUMENTATION PAGE

*Form Approved*
*OMB No. 0704-0188*



| 1. REPORT DATE *(DD-MM-YYYY)* | 2. REPORT TYPE | 3. DATES COVERED (From - To) |
|---|---|---|
| November 2021 | Technical Note | September 2020 – September 2021 |

**4. TITLE AND SUBTITLE**
Method for Rapid Small-Scale Simulated Aluminum Alloy Castings

**5a. CONTRACT NUMBER**

**5b. GRANT NUMBER**

**5c. PROGRAM ELEMENT NUMBER**

**6. AUTHOR(S)**
Taylor Cain and Jon-Erik Mogonye

**5d. PROJECT NUMBER**

**5e. TASK NUMBER**

**5f. WORK UNIT NUMBER**

**7. PERFORMING ORGANIZATION NAME(S) AND ADDRESS(ES)**
DEVCOM Army Research Laboratory
ATTN: FCDD-RLW-MF
Aberdeen Proving Ground, MD 21005

**8. PERFORMING ORGANIZATION REPORT NUMBER**
ARL-TN-1091

**9. SPONSORING/MONITORING AGENCY NAME(S) AND ADDRESS(ES)**

**10. SPONSOR/MONITOR'S ACRONYM(S)**

**11. SPONSOR/MONITOR'S REPORT NUMBER(S)**

**12. DISTRIBUTION/AVAILABILITY STATEMENT**
Approved for public release: distribution unlimited.

**13. SUPPLEMENTARY NOTES**
ORCID IDs: Taylor Cain, 0000-0002-6621-914X; Jon Erik-Mogonye, 0000-0002-7508-083X

**14. ABSTRACT**
A method for rapid small laboratory-scale production of aluminum alloys was evaluated for its ability to provide industrially relevant solidification rates. The results of this study have validated the button melting method for suitable use to provide industrially relevant solidification rates and resulting microstructure. Buttons produced using this method are expected to provide rapid discovery and selection of novel aluminum alloys.

**15. SUBJECT TERMS**
aluminum alloy, casting, solidification rate, dendrite arm spacing, metallurgy

| 16. SECURITY CLASSIFICATION OF: | | | 17. LIMITATION OF ABSTRACT | 18. NUMBER OF PAGES | 19a. NAME OF RESPONSIBLE PERSON |
|---|---|---|---|---|---|
| a. REPORT | b. ABSTRACT | c. THIS PAGE | | | Taylor Cain |
| Unclassified | Unclassified | Unclassified | UU | 16 | 19b. TELEPHONE NUMBER (Include area code) (410) 278-3162 |

Standard Form 298 (Rev. 8/98)
Prescribed by ANSI Std. Z39.18

## Contents

## List of Figures



## List of Tables

# 1. Introduction

The practice of melting and casting alloys has been of great importance to civilization since the Bronze Age and has seen significant advancements in melt treatment and quality, mold design, and casting methods leading to the production of highly repeatable, high-quality castings. Products made from castings take two forms: (1) where the metal is cast into its final net shape or near net shape with minimal required additional processing and (2) metal cast into large ingots that are subject to mechanical work by rolling, extruding, forging, or other processing methods. Both types of products are widely used within the Army and form the bulk structure of ground and air vehicle and weapons systems.

Shape castings are produced by a number of different methods all of which provide varying combinations of solidification behavior, surface finishes, maximum/minimum size, and geometric tolerances that need to be factored into meeting the required physical properties of a part. Throughout history, the most relevant types of castings have been sand castings, investment castings, permanent mold castings, and die castings. Sand castings have the slowest solidification rates of typically less than 0.3 °C/s, while permanent mold castings solidify between approximately 0.1 and 0.5 °C/s, and die castings are the fastest at about 16–56 °C/s.[1] While there are other methods for rapid solidification leading to unique material properties, this range of solidification rates is the most industrially relevant for design of novel high-performance alloys.

The landscape of alloy development has been changing at a rapid pace as technological advancements continue. In particular, additive manufacturing and computational engineering have led the push for high-throughput alloy production and characterization. The aim of this study is to evaluate the feasibility of a small-scale melting method aimed at rapid production of alloys that can be used to screen large compositional arrays in design of novel aluminum (Al) casting alloys with the desired output of providing industrially relevant processing conditions for facile product transition. Here, a small laboratory-scale vacuum induction melting furnace is used to melt well-known Al casting alloy A356.0 while measuring the solidification rate under various cooling conditions. The resultant microstructures were then analyzed for grain size and correlated to the solidification rate to provide a constitutive relationship between the grain size and cooling rate in comparison with industrial castings.

## 2. Experimental Procedures

In this investigation, a 25-kW vacuum induction melting (VIM) furnace with an output frequency of 30–80 kHz was used for all melting operations. Samples were melted inside a quartz tube, vacuum flange assembly as shown by the schematic image in Fig. 1. The quartz tube was lined with a porous $Al_2O_3$ refractory that insulated the quartz tube from a graphite-melting crucible. A 35-mm-diameter dense graphite crucible with a wall thickness of 5 mm was loaded with varying masses of aluminum alloy A356.0 (UNS A03560, Al-7Si) while a graphite sheathed thermocouple was centered in the melt pool at a depth of 50% of the height of the melt.

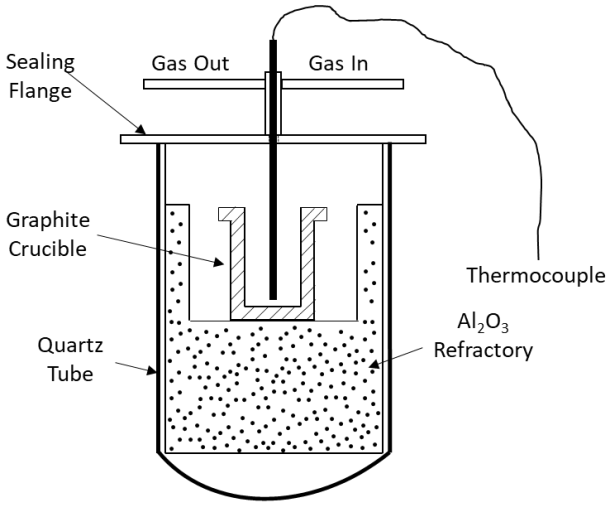


**Fig. 1 Quartz tube with vacuum flange assembly for melting Al alloys**

Prior to heating, the quartz tube assembly was evacuated under vacuum and backfilled with ultra-high purity (99.999%) helium (He) three times to remove oxygen from the chamber and provide an He environment. During heating, the temperature of the graphite crucible was raised at approximately 145 °C/min until the desired holding temperature of 750 °C was reached. The melt was then held at 750 °C ± 5 °C for 5 min via pulsing of the induction current on and off to ensure full melting of alloy A356.0 whose liquidus and solidus temperatures are 615 °C and 555 °C, respectively.[2] After the 5-min hold, the induction power was turned off and the alloy was allowed to cool within the furnace and solidify while the temperature was recorded via an eight-channel USB Omega acquisition module at four data points per second. The sample was allowed to cool to approximately 500 °C twice under positive flow of He gas at a pressure of +0.01 bar followed by two melting and cooling cycles under a vacuum of –0.1 bar on separate samples each

weighing 22.46 g. A third sample weighing 92.50 g was cooled under a vacuum of –0.1 bar to provide a third unique cooling rate.

Solidified samples were sectioned and polished to a final finish using a 0.25-µm diamond oil-based suspension such that the polished surface was representative of the cross-sectional area where the thermocouple was placed in the melt pool. After final polishing, samples were etched to reveal grain structure using 10 g/L NaOH solution at room temperature. Secondary dendrite arm spacing (SDAS) was determined by measuring the distance between the centers of secondary dendrite arms parallel to the primary dendrite arm and counting the number of secondary dendrite arms along the distance as shown in Fig. 2. Secondary dendrite arm spacing was then determined by

$$d = \frac{L}{N-1} \tag{1}$$

where $d$ is the SDAS, $L$ is the length of the dendrite, and $N$ is the number of secondary dendrite arms counted along $L$. Here, a center-to-center measurement was deemed more accurate than an interface-to-interface measurement as the interfacial boundaries can be distorted from etching.

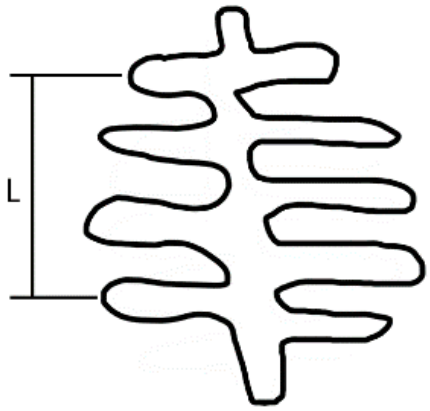


**Fig. 2 Schematic of SDAS measurement where the distance *L* is measured from the center-to-center distance of secondary dendrite arms**

## 3. Results

The measured cooling rate of alloy A356.0 under varying solidification conditions is shown in Fig. 3, where three distinct cooling rates were measured for the 22.46-g sample under He gas flow (He gas-1), the 22.46-g sample under vacuum (Vacuum-1), and the 92.50-g sample under vacuum (Vacuum-2); the measured solidification rate by linear fitting of the steady-state linear region of the data between the solidus and liquidus is shown in Table 1. The measured solidification

rates are consistent with those of permanent mold castings, which is an important finding and revealed that the proposed button melting method can successfully simulate industrially relevant solidification rates with low quantities of metal. Furthermore, the total batch time from loading the quartz crucible with material to safe removal temperature of a completed melt is approximately 45 min, which provides a moderately rapid turnaround for producing buttons of different compositions with a single VIM in a workday. Such capability can then be used to rapidly screen promising compositions on a lab scale using a variety of characterization techniques.

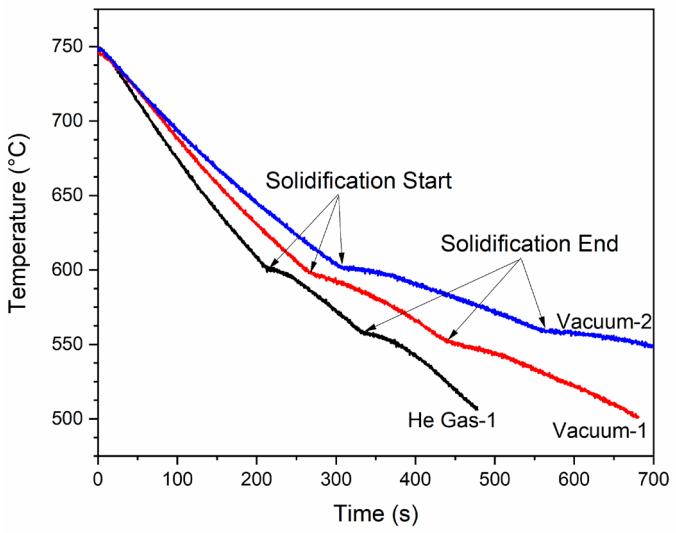


**Fig. 3 Measured cooling rate vs. time for A356.0 under vacuum and positive flow of He gas**

**Table 1 Solidification rate of A356.0 under vacuum and positive flow of He gas**

| Solidification condition | Steady-state solidification rate (°C/min) |
|---|---|
| He Gas-1 | 0.43 |
| Vacuum-1 | 0.29 |
| Vacuum-2 | 0.19 |

Representative optical micrographs of the solidified structure of each cooling condition are shown in Fig. 4. Measurements of SDAS are shown in Table 2 and are plotted with their corresponding solidification rate in Fig. 5, where the ordinate and abscissa are logarithmic scale. Linearization of the data in this manner provides a power law relationship between SDAS and cooling rate following

$$d = b(SR)^{-n} \quad (2)$$

where *SR* is the solidification rate, *b* and *n* are constants related to thermal variables of the solidification process, and *n* is typically near one-third for SDAS and one-half for primary dendrite spacing of Al alloys.[3] Fitting of the data collected in this experiment provided a value of *n* approximately equal to 0.4, which is within reason for SDAS for Al alloys. However, the value of *b* varies greatly from values measured in the literature. For example, Spear and Gardner[4] and Wang and Caceres[5] found values of 39.4 and 41.6, respectively, as compared to 1.136 in this study. The implication of this deviation is that the measured SDAS is much smaller than it should be for the measured solidification rate, but the *n* value near one-third shows that the change in solidification rate under each solidification condition provides a similar order of magnitude range change in solidification rate with SDAS as those values established in literature. It is possible that the origin of this deviation in *b* is due to the graphite sheath used to protect the thermocouple from reactive degradation with the melt pool. While graphite has a nominally high thermal conductivity compared to Al, the sheath would act as a thermal barrier to slow the rate of heat transfer between the melt and the thermocouple, thus underestimating the solidification rate. Indeed, the results of Spear and Gardner[4] and Wang and Caceres[5] indicate that the solidification rate determined here is slower by a factor of about 20, meaning that the solidification rate of button melts is between that of permanent mold castings and die castings. Thus, acceptance of solidification rates based on the values determined by those two studies still validates the button melt method for its suitability to simulate industrially relevant solidification rates.

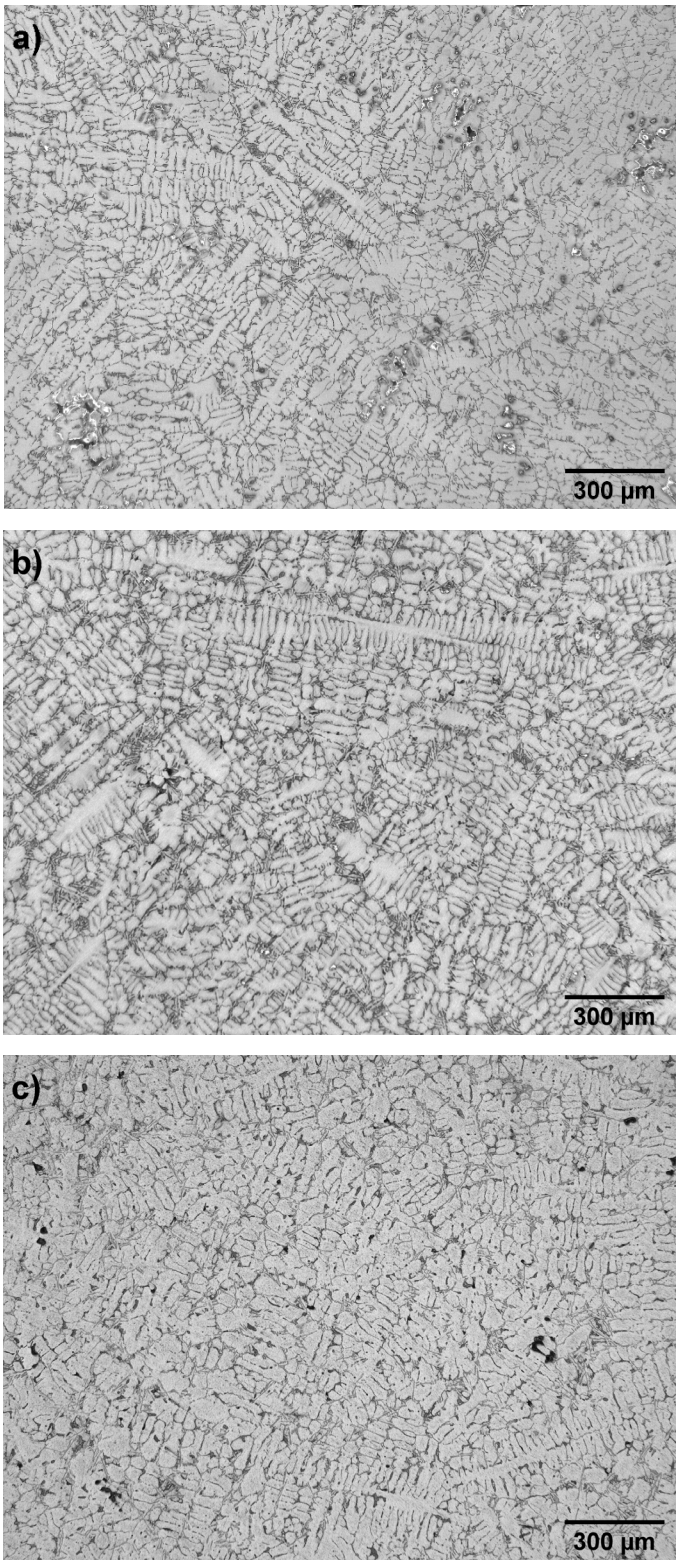


**Fig. 4 Representative optical images of the 22.46-g A356.0 melt cooled under (a) He, (b) vacuum, and (c) 92.50-g A356.0 melt cooled under vacuum**

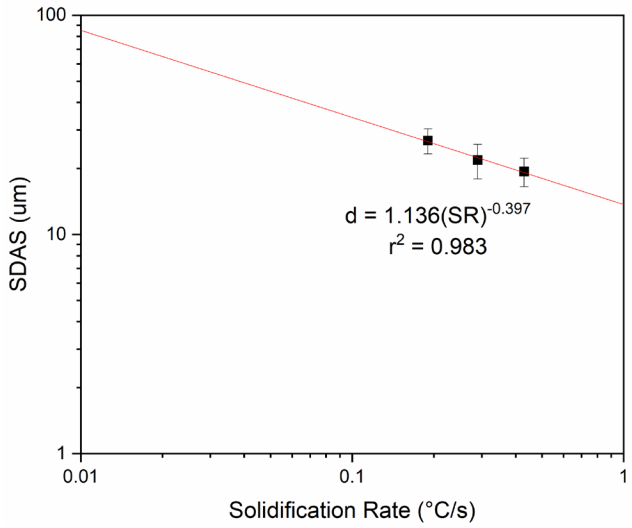


**Fig. 5 A plot of SDAS vs. solidification rate with the log-log fit of the measured data**

**Table 2 Measured SDAS for each solidification condition**

| Solidification condition | SDAS (μm) |
|---|---|
| He Gas-1 | 19.39 ± 2.89 |
| Vacuum-1 | 21.83 ± 3.93 |
| Vacuum-2 | 26.79 ± 3.51 |

## 4. Conclusions

A method for producing small-scale Al alloys to mimic industrial castings via melt processing was proposed. The results showed that the solidification rate of A356.0 is consistent with industrially relevant casting methods, which validated the proposed method for use on the laboratory scale for rapid novel alloy development.

## 5. References


1. Weiss D. Advances in the sand casting of aluminium alloys. In: Lumley RN, editor. Fundamentals of aluminium metallurgy. Woodhead Publishing; 2018. p. 159–171.
2. 356.0 and A356.0[1]: Al-Si-Mg high-strength casting alloys. In: Anderson K, Weritz J, Kaufman JG, editors. Properties and selection of aluminum alloys. ASM International; 2019.
3. Flemmings MC. Solidification processing. McGraw-Hill; 1974.
4. Spear RE, Gardner GR. Trans Am Fndrymn Soc. 1963;71:209.
5. Wang QG, Caceres CH. Mg effects on the eutectic structure and tensile properties of Al-Si-Mg alloys. Mat Sci Forum. 1997;242:156–164.

## List of Symbols, Abbreviations, and Acronyms

| | |
|---|---|
| Al | aluminum |
| He | helium |
| SDAS | secondary dendrite arm spacing |
| VIM | vacuum induction melting |

| | |
|---|---|
| 1 (PDF) | DEFENSE TECHNICAL INFORMATION CTR DTIC OCA |
| 1 (PDF) | DEVCOM ARL FCDD RLD DCI TECH LIB |
| 2 (PDF) | DEVCOM ARL FCDD RLW MF T CAIN<br>FCDD RLW VA J ERIK-MOGONYE |